Langmuir

Article

pubs.acs.org/Langmuir

Supramolecular Self-Assembly Induced Graphene Oxide Based Hydrogels and Organogels

Qian-Yi Cheng,[†,‡] Ding Zhou,[†] Yun Gao,[†] Qi Chen,[†] Zhong Zhang,*[,†] and Bao-Hang Han*[,†]

[†]National Center for Nanoscience and Technology, Beijing 100190, China

[‡]College of Chemistry and Molecular Engineering, Peking University, Beijing 100871, China

Supporting Information

ABSTRACT: We demonstrate the construction of three-dimensional graphene oxide based gel networks through the self-assembly of a series of amphiphilic molecules, which possess a polar carbohydrate headgroup attached to a nonpolar pyrene group. The gelation process can occur in both aqueous and organic solutions and be influenced by the gelators' molecular structure. The driving forces for the gelation process were determined as $\pi-\pi$ stacking and hydrogen bonding interaction by using fluorescence and infrared spectroscopies. Rheometry was used to investigate the mechanical properties of the hydrogels and the organogels. The hydrogel was investigated to be applied to remove dye from aqueous solution.

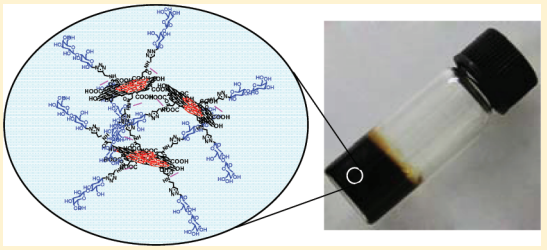

INTRODUCTION

Graphene oxide (GO) sheet, a two-dimensional carbon nanostructure of one atom thickness, is generally prepared from graphite through chemical oxidation and exfoliation process.[1,2] Because it has plenty of hydrophilic oxygenated groups, it is easily functionalized through covalent grafting and easily well-dispersed in water and many polar organic solvents.[3,4] Meanwhile, the hydrophobic domain of GO sheets provides an easy way for their noncovalent functionalization with aromatic and/or hydrophobic molecules. GO was used by Ruoff and co-workers in 2006 as an important component to construct functional composites after covalent functionalization.[5] From then on, various GO composites have been prepared using different kinds of linkers, such as organic molecules,[6] polymers,[7,8] metal oxides,[9,10] and metal nanoparticles,[11] which were reported to show great potential in applications, such as catalysis,[11] supercapacitors,[10] drug delivery,[8] and energy storage.[9] Some studies focusing on the solution properties of GO and the self-assembling behaviors of GO sheets have been reported recently. For example, our group reported a supramolecular hydrogel based on triblock copolymer modified graphene sheets and α-cyclodextrin, which show a potential in drug delivery and controlled release systems.[7] The GO composite hydrogels were formed by GO/PVA solution[8] and GO/DNA solution,[12] which show a potential capacity for pH controlled selective drug release and dye adsorption, respectively. A high-performance self-assembled graphene hydrogel was prepared by a one-step hydrothermal method with excellent mechanical, thermal, and electrochemical properties.[13] The driving forces for the gelation process of GO sheets are reported as hydrogen bonding, $\pi-\pi$ stacking, electrostatic, and van der Waals interactions.[8] However, to the best of our knowledge, work on the GO supramolecular gels through the noncovalent intermolecular interactions between the carbohydrate derivatives has not been reported yet.

Carbohydrates are some of the most significant natural biomolecules, which govern numerous critical biological processes, such as inflammation, bacterial and viral infections, cell growth and recognition, and immune response.[14−18] They can be used as building blocks of the low molecular weight gelators (LMWGs) on account of their special structure and biological properties. LMWGs form gels in solvents with solvent molecules as major components (usually more than 95 wt %), through noncovalent interactions, such as hydrogen bonding, van der Waals, and $\pi-\pi$ stacking interactions.[19,20] They were reported to show great potential in various applications, such as catalysis,[21] tissue engineering,[22] pollutant absorbents, and drug or gene release.[23] The self-assembling property of LMWGs was employed to fabricate carbon nanotube gels. As reported, the mechanical and electrical properties of LMWGs are significantly improved through incorporating with carbon nanotubes.[24,25] However, to date, there has been little work reported on GO supramolecular gels formed through LMWGs.[26] Herein we develop a method to prepare GO hydrogels and organogels through supramolecular self-assembly of amphiphilic molecules, which have a polar carbohydrate headgroup attached to a nonpolar pyrene group. GO sheets form a gel network mainly through hydrogen bonding and $\pi-\pi$ stacking interactions with the glycoconjugate based gelators in both aqueous and organic solutions. The influence of differences in the structure of the LMWGs on the gelation behavior of GO suspension was also studied.

Received: November 19, 2011
Revised: January 9, 2012
Published: January 14, 2012

   dx.doi.org/10.1021/la204558f | *Langmuir* 2012, 28, 3005−3010

Scheme 1. Synthetic Routes to Gelators

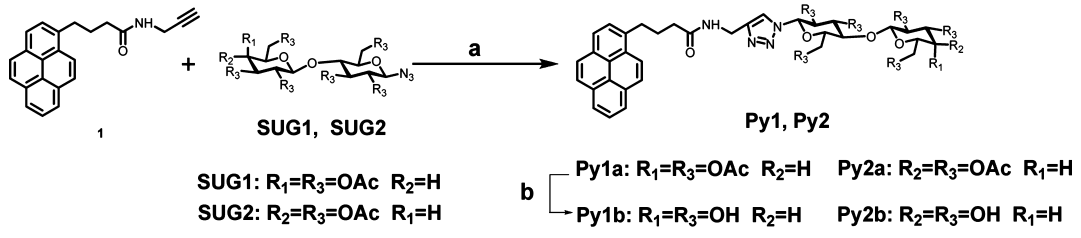

a) $CuSO_4 \cdot 5H_2O$, ascorbate sodium, H_2O/THF, 60 °C, 6 h b) NaOMe, MeOH rt. 3 h

Yields: Py1a, 65 %; Py2a, 61 %; Py1b, 72 %; Py2b, 73 %

EXPERIMENTAL SECTION

Materials. Natural flake graphite (average particle diameter of 20 μm, 99 wt % purity) was obtained from Yingshida Graphite Co. Ltd. (Qingdao, China). Sulfuric acid (98 wt %), sodium nitrate, *N*,*N*-dimethylformamide (DMF), and hydrogen peroxide (30 wt %) were purchased from Beijing Chemical Works, China. 1-Pyrenebutyric acid (>99.0%) was purchased from Sigma-Aldrich. Basic fuchsine (A.R.) was purchased from Jinke Research Institute of Fine Chemicals (Tianjin, China). All these chemicals were used without further purification. 1-*N*-(Propin-3-yl)-4-(pyren-1-yl)butyramide (**1**)[27] and the sugar intermediates per-*O*-acetylated-β-D-lactopyranosyl azide (SUG1) and per-*O*-acetylated-β-D-cellopyranosyl azide (SUG2) were prepared according to reported procedures, respectively.[28,29] Ultrapure water (18.2 MΩ cm) used throughout all experiments was produced by a Millipore system (Millipore, USA).

Instrumental Characterization. The ^1H and ^{13}C NMR spectra were recorded on a Bruker DMX400 NMR spectrometer. Mass spectra were acquired with a Bruker Microflex LRF MALDI-TOF mass spectrometer. Infrared (IR) spectra were obtained in KBr pellets using a Spectrum One Fourier transform infrared (FT-IR) spectrometer (Perkin-Elmer Instruments Co. Ltd.). Thermogravimetric analyses (TGA) were performed on a Pyris Diamond thermogravimetric/differential thermal analyzer (5 °C min^{-1}, nitrogen). Ultraviolet−visible (UV−vis) spectra were measured using a Perkin-Elmer Lamda 950 UV−vis−NIR spectrophotometer and quartz cells with 1 cm path length. The fluorescence spectra were measured in a 1 cm path length cell using a Perkin-Elmer LS55 luminescence spectrometer. Scanning electron microscopy (SEM) images were observed on a Hitachi S-4800 scanning electron microscope at an accelerating voltage of 6 kV. Atomic force microscopy (AFM) images were taken in tapping mode with a Dimension 3100 atomic force microscope and Nanoscope IVa NS4a controller (Veeco Instruments Inc., USA). Rheological studies were performed on a HAAKE MARS II modular advanced rheometer system.

Synthesis: General Synthesis Procedure for Gelators. The synthetic routes to the gelators are outlined in Scheme 1. To a mixture of **1** (112 mg, 0.5 mmol) and SUG1 or SUG2 (396 mg, 0.6 mmol) in water−terahydrofuran (1:2, 15 mL), freshly prepared aqueous sodium ascorbate (1.0 M, 0.15 mmol) and copper sulfate (0.5 M, 0.075 mmol) were added. The heterogeneous mixture was stirred vigorously at 60 °C until complete consumption of the reactants occurred based on TLC monitoring. Water (20 mL) was added and the product was extracted with ethyl acetate (3 × 25 mL). The combined organic phase was dried over anhydrous sodium sulfate and evaporated in vacuo. The crude product was subjected to column chromatography to give **Py1a** (320 mg) or **Py2a** (300 mg) as a yellow solid.

The acetylate-protected **Py1a** or **Py2a** (320 mg) was added to a solution of dry dichloromethane (5 mL) and methanol (10 mL) followed by addition of sodium methoxide/methanol solution (1.0 M, 0.25 mL). The reaction mixture was stirred at room temperature for 3 h. Acid resin was added into the mixture until the pH value reached 7. The mixture was filtrated and evaporated in vacuo to give the product *N*-(β-D-lactopyranosyl)-1*H*-1,2,3-(triazole-4-yl)methyl-4-(pyren-1-yl)-butyramide **Py1b** (162 mg) or *N*-(β-D-cellopyranosyl)-1*H*-1,2,3-(triazole-4-yl)methyl-4-(pyren-1-yl) butyramide **Py2b** (165 mg) as a yellow solid. The NMR data and MALDI-TOF mass spectra (Figure S1) of **Py1a**, **Py1b**, **Py2a**, and **Py2b** are provided in the Supporting Information.

Preparation of GO Dispersions in Water and DMF. GOs were prepared by chemical exfoliation of the natural flake graphite by the modified Hummers method.[1,2,7] GO dispersion in DMF was obtained by a solvent exchange method from the as-exfoliated aqueous GO dispersion.[2,30] Aqueous GO dispersion was subjected to the centrifugation tube and centrifuged at 11 000 rpm for 30 min, the supernatant liquid was removed, and the GOs were redispersed in DMF. The process was repeated five times.

Preparation of GO Hydrogels. Aqueous **Py1b** or **Py2b** solution was added into aqueous GO dispersion to reach the final concentrations of **Py1b** or **Py2b** (10.0 mg mL^{-1}) and GO (4.0 mg mL^{-1}), and the mixture was heated and stirred at 70 °C for 30 min to make the **Py1b** or **Py2b** well distributed. After standing at room temperature for 30 min, the mixture was sonicated for 1 h to form the hydrogel GPG1 or GPG2. The hydrogel formation was confirmed by a tube inversion method.

Preparation of GO Organogels. **Py1b** or **Py2b** solution in DMF was added into GO dispersion in an organic solvent to reach the final concentrations of **Py1b** or **Py2b** (10.0 mg mL^{-1}) and GO (4.0 mg mL^{-1}), and the mixture was heated and stirred at 70 °C for 30 min to make the **Py1b** or **Py2b** well distributed. This was followed by standing at room temperature for 30 min to form the organogel GPG3 or GPG4. The formation of the organogel was confirmed by a tube inversion method.

Removal of Basic Fuchsine from Aqueous Solution. After 1.0 mL of hydrogel was formed and kept at room temperature for at least 1 h, aqueous basic fuchsine solution (1.0 mg mL^{-1}, 1.0 mL) was added on the top of the hydrogel GPG1. At predetermined time internals, 10 μL of the solution at the upper layer was taken out and diluted for measurement by UV−vis spectroscopy to determine the concentration of basic fuchsine remaining using the absorption peak at 543 nm.

RESULTS AND DISCUSSION

The as-prepared GO sheets show one atom thickness and several hundred nanometers to several micrometers in size (Figure S2 in the Supporting Information). The supramolecular hydrogel was fabricated by mixing the gelators and aqueous GO dispersion through stirring and heating followed by sonication treatment to complete the gelation process. During the heating and stirring processes, the gelators were completely dissolved in GO dispersion without any aggregation. After sonication, the mixture was allowed to stand at room temperature for several hours, and then the dark brown GO dispersion turned into a light brown hydrogel confirmed by a tube inversion method (Figure 1a). In the heating process, the gelators attached to the GO sheets through π−π stacking interaction. After cooling to room temperature and sonication treatment, the hydrogen bonds between the GO sheets and gelators help the formation of the GO hybrid gels (Figure 2). If the mixture was allowed to stand at 50 °C for several hours after the heating process, the

dx.doi.org/10.1021/la204558f | *Langmuir* 2012, 28, 3005−3010

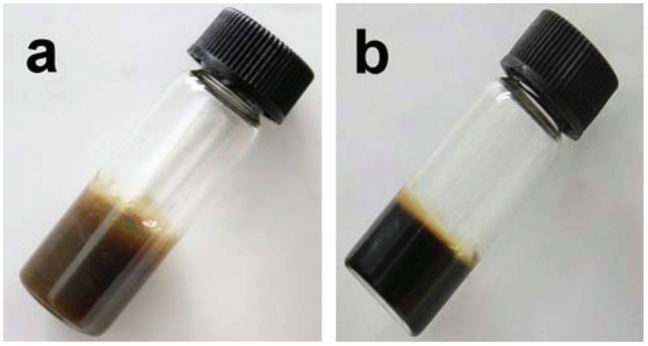

Figure 1. Images of (a) hydrogel GPG1 and (b) organogel GPG3 in DMF.

GO dispersion still maintained its fluidity. To prove the gelation process happened between the GO sheets and gelators, we used the aqueous gelator solution at the same concentration as control experiment. At the same concentration of gelator without the GO, white fiberlike self-assemblies formed in the aqueous solution instead of hydrogel after being heated and sonicated as the SEM image showed (Figure S3a in the Supporting Information), which is due to the strong $\pi-\pi$ stacking interaction between the pyrene groups (Figure 2). This result proves that the GO sheets and gelators are both integrant in the gelation process. Since the as-prepared amphiphilic molecules can also be dissolved in organic solvent, we tried to fabricate GO organogel as well. GO organogels were prepared in DMF, in which GO shows a good dispersibility (Figure 1b). The gelator of the same concentration as in DMF without the GO was also used as control experiment; no organogel was obtained either. The mixture of GO sheets and gelators possesses a very strong gelating ability. The total content of the solvent in gels is about 98.6 wt %; i.e., the content of the GO and the gelator is only about 1.4 wt %. Lower concentrations of gelator and GO dispersion are not good for the formation of gels.

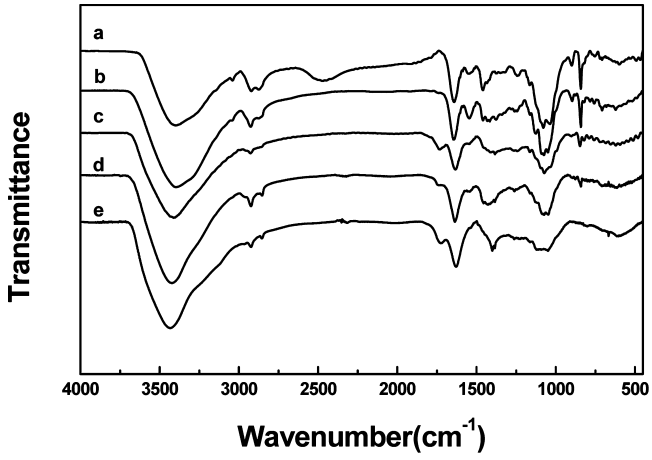

Figure 3. IR spectra of **Py2b** (a), **Py1b** (b), freeze-dried GPG2 (c) and GPG1 (d), and powdery GO (e).

The possible driving force for the gelation process is partially attributed to the $\pi-\pi$ stacking interaction existing between pyrene groups of the amphiphilic **Py1b** or **Py2b** and GO surface (Figure 2), evidenced by fluorescence spectra of

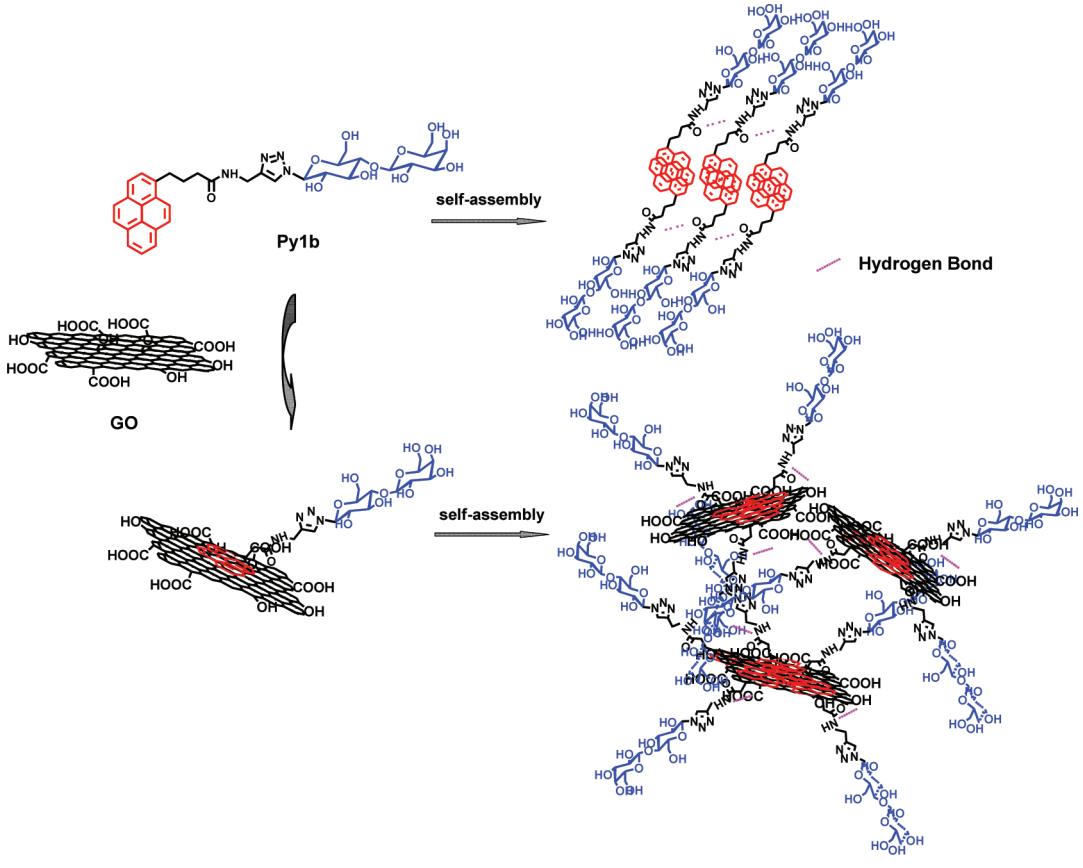

Figure 2. Schematic representation of the GO hybrid gel formation.

dx.doi.org/10.1021/la204558f | *Langmuir* 2012, 28, 3005−3010

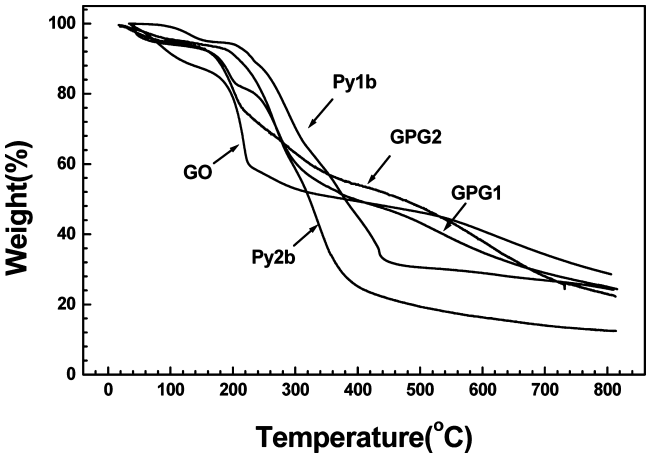

Figure 4. TGA thermograms of powdery GO, **Py1b**, **Py2b**, and freeze-dried GPG1 and GPG2.

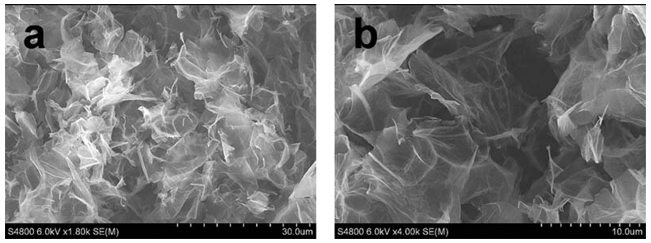

Figure 5. SEM images of morphologies of the freeze-dried hydrogel GPG1 at low (a) and high (b) magnification.

aqueous **Py1b** solution in the absence and presence of GO dispersion at various concentrations. The fluorescence emission at 360−430 nm of aqueous **Py1b** solution decreases gradually with stepwise addition of GO dispersion at 25 °C (Figure S4 in the Supporting Information), which indicates that $\pi-\pi$ stacking interaction exists between the molecule **Py1b** and the surface of GO sheets. Such an interaction may accelerate their self-assembly process, thereby strengthening the gel and leading to reinforced supramolecular architectures.

Hydrogen bonds among −OH and −CO−NH− groups in **Py1b** or **Py2b** and −OH and −COOH groups on GO surface contribute as another kind of driving force in the gelation process, which are demonstrated by the IR spectra of freeze-dried GO based hydrogels compared to that of **Py1b** or **Py2b**. The IR spectra of freeze-dried GO, hydrogels, and bulk **Py1b** and **Py2b** are shown in Figure 3. The spectra of the bulk **Py1b** and **Py2b** (Figure 3, traces a and b) show characteristic adsorption bands corresponding to the stretching vibration (sv) of N−H's of the amide groups at 3399 cm^{-1}, the stretching vibration of carbonyls of the amide groups (amide I band, 1600−1700 cm^{-1}) at 1641 cm^{-1}, and the bending vibration (bv) of N−H's of the amide groups (amide II band, 1460−1554 cm^{-1}) at 1552 cm^{-1}, while the freeze-dried GO shows the stretching vibration of O−H groups at 3434 cm^{-1} (Figure 3, trace e).[31] For freeze-dried hydrogels (Figure 3, traces c and d), the amide groups of gelators and the O−H groups of GO were involved in hydrogen bonding, which was demonstrated by the characteristic peak shifts to lower wavenumbers as sv and bv peaks of amide at 1633 and 1547 cm^{-1} and the sv peak of O−H and N−H at 3411 cm^{-1}.

Freeze-dried GO and hydrogel samples were further analyzed using TGA (Figure 4) by heating the samples under a nitrogen

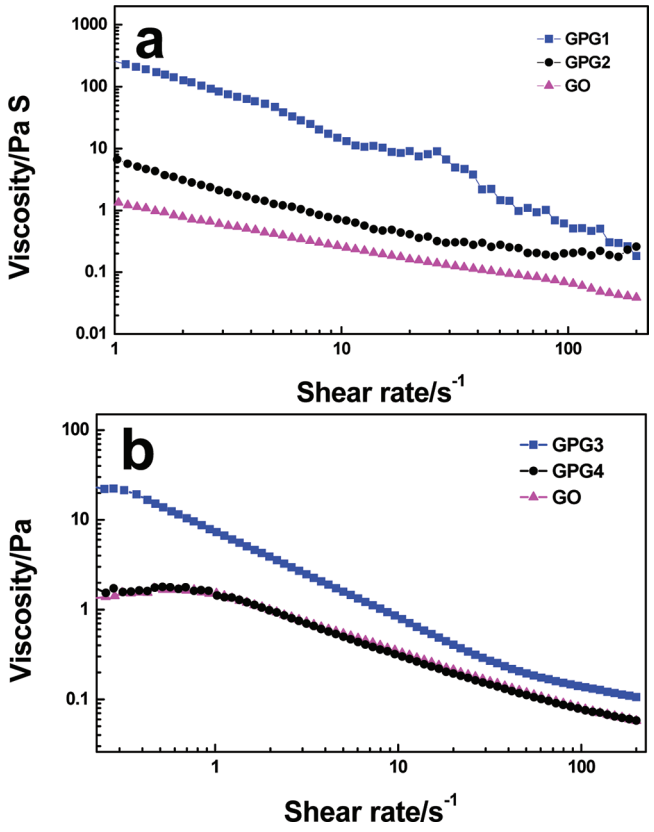

Figure 6. Steady rheological behaviors of (a) GO (triangles) and hydrogels GPG1 (squares) and GPG2 (circles), and (b) GO (triangles) and organogels GPG3 (squares) and GPG4 (circles) in DMF.

atmosphere from room temperature to 800 °C. The curve of freeze-dried GO shows about 10% weight loss at ca. 100 °C due to evaporation of water molecules that are held in the material. The significant weight loss (30%) is observed from 160 to 220 °C, due to the removal of the functional groups (−OH and −COOH) from the GO. The curves of freeze-dried hydrogels exhibit a little weight loss corresponding to water evaporation and 10% weight loss at 180 °C due to the decomposition of the amide carbonyl group, which shows less thermal stability compared with $-COO^{-}$ groups. The freeze-dried hydrogels show a difference in the onset temperature compared with GO, indicating that new chemical interactions are formed between the GO and **Py1b** or **Py2b**.

In order to gain a better insight into the microstructures of the composites, the morphologies of the freeze-dried hydrogels were observed by SEM. The SEM images of the freeze-dried hydrogel GPG1 are shown in Figure 5. Images of freeze-dried hydrogels prepared from the **Py1b** and GO in water exhibit a loose network structure and a lamellar structure indicating the leakage or removal of the trapped solvent molecules during the freeze-drying. The GO sheets in freeze-dried hydrogel exhibit very thin layerlike structures, which coalesced through gelators as cross-linking agents resulting in a three-dimensional porous network. The morphology of powdery GO sheets looks like thicker than freeze-dried hydrogels due to the aggregation of GO sheets during the freeze-drying process (Figure S3b in the Supporting Information). The morphology of self-assemblies of gelators at the same concentration exhibits a fiberlike structure as shown in Figure S3a in the Supporting Information. This

dx.doi.org/10.1021/la204558f | *Langmuir* 2012, 28, 3005−3010

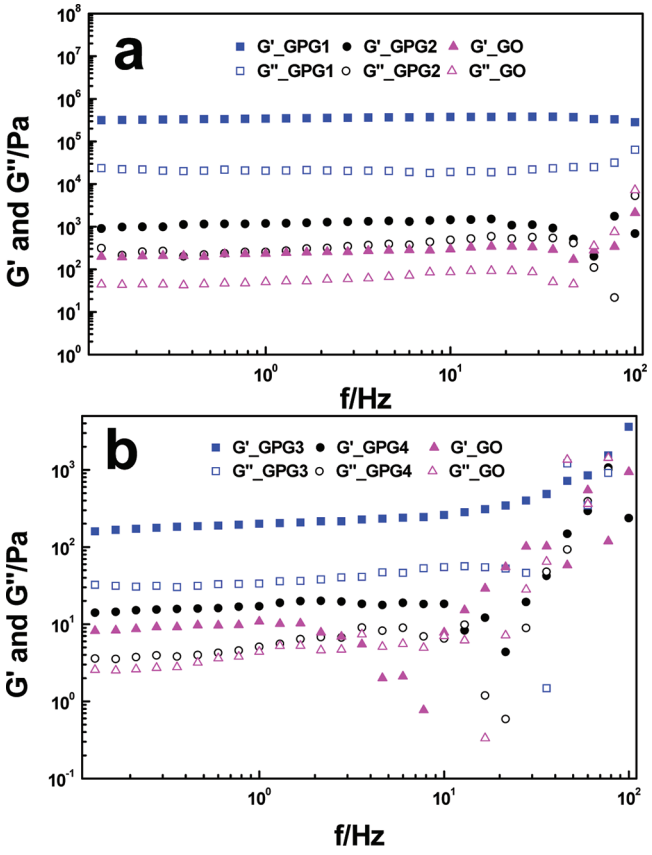

Figure 7. Dynamic rheological behaviors (G', solid symbols; G'', open symbols) of (a) GO (triangles) and hydrogels GPG1 (squares) and GPG2 (circle), and (b) GO (triangles) and organogels GPG3 (squares) and GPG4 (circles) in DMF at 25 °C with strain amplitude (γ) at 0.002.

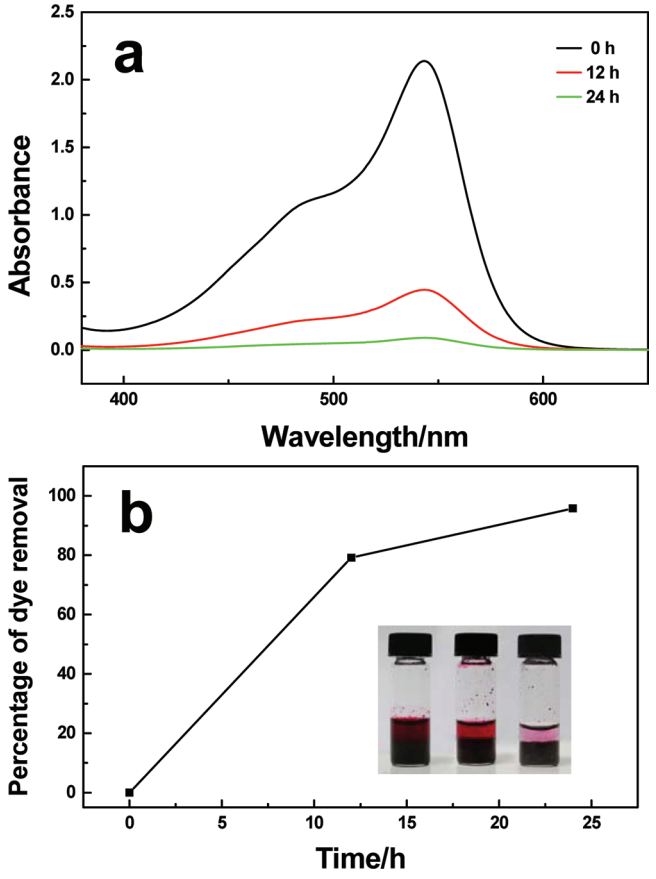

Figure 8. (a) Absorption spectra of aqueous basic fuchsine solution on the top of hydrogel GPG1. (b) Percentages of dye removal by the hydrogel GPG1 at different times; the inset shows the digital images of dye removal (at 0, 12, and 24 h from left to right).

difference can be attributed to the strong $\pi-\pi$ stacking between the pyrene groups in aqueous solution as supported by the fluorescence spectra of the aqueous gelator solution at different concentrations, in which a fluorescence peak at a longer wavelength of 480 nm at a higher concentration was observed (Figure S5 in the Supporting Information) corresponding to the excited-state dimer of pyrene rings.

The mechanical properties of the GO-containing hydrogels, organogels, and GO suspension samples were characterized by steady mechanical rheometry at 25 °C shown in Figure 6. The viscosity of the gel samples greatly diminishes as they are sheared, which is a typical characteristic of supramolecular gels with physical cross-linking. Compared to the GO suspension, the viscosity of the supramolecular gels with 1.0 wt % **Py1b** significantly increases; meanwhile, the addition of **Py2b** does not cause that much change in both water and DMF systems.

The dynamic rheological behaviors of GO-containing gel samples and GO were measured by applying the oscillating strain (γ) at 0.2% as a function of frequency (f) shown in Figure 7. The storage modulus G' and loss modulus G'' curves of the hydrogels and organogels are greater than the corresponding G' and G'' curves of the GO dispersion, illustrating that the **Py1b** and **Py2b** influence the elastic properties of the GO. Furthermore, the G' values of both hydrogel GPG1 and organogel GPG3 show a substantial elastic response and are larger than the G'' values over the entire angular frequency range. This result demonstrates that both the hydrogel and organogel possess a network structure. The ratio of G' to G'' for hydrogel GPG1 is 19.41, while that of the GO is 3.46, indicating enhanced stability and elastic response of the hydrogel GPG1. Like the results from the steady mechanical rheometry, the dynamic rheological behaviors of **Py2b**-containing gels in aqueous and DMF phases are relatively poor. The rheological results show that the incorporation of **Py1b** in the GO sheet suspension remarkably increases the elastic modulus, the viscous modulus, and the ultimate strength.

The reason for the contrast of mechanical behaviors induced by different gelators may be attributed to the difference in the molecular structure. Since both molecules have a carbohydrate group attached to a pyrene group through triazole and amide moieties, the only difference in the molecular structure is the configuration of the hydroxyl groups in the carbohydrate moiety. As reported, the configuration of the hydroxyl groups in the headgroup has an effect on the mesophase stability and clearing point.[32,33] Therefore, we hypothesize that the contrast of mechanical properties is due to the different configuration of the hydroxyl group of the gelators.

The dye-loading properties of the obtained supramolecular hydrogel were studied using basic fuchsine as the model dye. Aqueous dye solution (1.0 mg mL^{-1}, 1.0 mL) was added onto the top of GPG1 (1.0 mL) at room temperature. From absorption spectra (Figure 8a) and the digital images (Figure 8b, inset), we can find that, after standing at room temperature for 12 h, about 80% of the dye was adsorbed by the hydrogel and this value increases to about 96% after 24 h. As reported, the GO hydrogels show negative charges while the dye

dx.doi.org/10.1021/la204558f | *Langmuir* 2012, 28, 3005−3010

molecules are positively charged; this results in the high dye-loading ability of the GO hydrogel.[12]

CONCLUSIONS

We have developed a supramolecular self-assembly method to prepare GO supramolecular gels through using the carbohydrate-based LMWGs as linkers. The driving forces for the gelation process are $\pi-\pi$ stacking and hydrogen bonding interactions, which can be attributed to the pyrene moiety, amide and triazole linkage, and carbohydrate groups of the gelators. Considering the nice dispersibility of GO and gelators in aqueous and organic solvents, both the hydrogels and organogels were fabricated successfully. Furthermore, the gelators' molecular structure shows an influence on the gelation process. If the D-lactopyranosyl residue of a gelator is replaced by a D-cellopyranosyl residue, the mechanical properties of the gels decrease obviously. The as-prepared GO hydrogel shows a nice dye-loading ability confirmed by using basic fuchsine as a model dye. This work describes the fabrication of three-dimensional GO self-assemblies with LMWGs, which will help in the rational design and preparation of functionalized graphene-based materials. Chemical and biological properties of GO and carbohydrates make the as-prepared GO gels show promising potential in catalysis, tissue engineering, pollutant absorbents, and biosensor applications.

ASSOCIATED CONTENT

Supporting Information

^{1}H and ^{13}C NMR data and mass spectra of **Py1a**, **Py1b**, **Py2a**, and **Py2b**, AFM image and cross-section analysis of as-exfoliated GO, SEM images of self-assemblies of **Py1b** and powdery GO, fluorescence spectra of aqueous **Py1b** solution with various concentrations of GO, and fluorescence spectra of **Py1b** in aqueous solution at different concentrations. This material is available free of charge via the Internet at http://pubs.acs.org.

AUTHOR INFORMATION

Corresponding Author

*Tel./fax: +86 10 8254 5586 (Z.Z.); +86 10 8254 5576 (B.-H.H.). E-mail: zhong.zhang@nanoctr.cn (Z.Z.); hanbh@nanoctr.cn (B.-H.H.).

ACKNOWLEDGMENTS

The financial support of the National Science Foundation of China (Grant 91023001) and the Ministry of Science and Technology of China (National Basic Research Program, Grants 2011CB932500 and 2012CB937503).

REFERENCES

(1) Hummers, W. S.; Offeman, R. E. *J. Am. Chem. Soc.* **1958**, *80* (6), 1339−1339.
(2) Hirata, M.; Gotou, T.; Horiuchi, S.; Fujiwara, M.; Ohba, M. *Carbon* **2004**, *42* (14), 2929−2937.
(3) Paredes, J. I.; Villar-Rodil, S.; Martínez-Alonso, A.; Tascón, J. M. D. *Langmuir* **2008**, *24* (19), 10560−10564.
(4) Compton, O. C.; Nguyen, S. T. *Small* **2010**, *6* (6), 711−723.
(5) Stankovich, S.; Dikin, D. A.; Dommett, G. H. B.; Kohlhaas, K. M.; Zimney, E. J.; Stach, E. A.; Piner, R. D.; Nguyen, S. T.; Ruoff, R. S. *Nature* **2006**, *442*, 282−286.
(6) Zhang, D.-D.; Zu, S.-Z.; Han, B.-H. *Carbon* **2009**, *47* (13), 2993−3000.
(7) Zu, S.-Z.; Han, B.-H. *J. Phys. Chem. C* **2009**, *113* (31), 13651−13657.
(8) Bai, H.; Li, C.; Wang, X. L.; Shi, G. Q. *Chem. Commun.* **2010**, *46* (14), 2376−2378.
(9) Zhou, D.; Han, B.-H. *Adv. Funct. Mater.* **2010**, *20* (16), 2717−2722.
(10) Chen, S.; Zhu, J. W.; Wu, X. D.; Han, Q. F.; Wang, X. *ACS Nano* **2010**, *4* (5), 2822−2830.
(11) Scheuermann, G. M.; Rumi, L.; Steurer, P.; Bannwarth, W.; Mülhaupt, R. *J. Am. Chem. Soc.* **2009**, *131* (23), 8262−8270.
(12) Xu, Y. X.; Wu, Q.; Sun, Y. Q.; Bai, H.; Shi, G. Q. *ACS Nano* **2010**, *4* (12), 7358−7362.
(13) Xu, Y. X.; Sheng, K. X.; Li, C.; Shi, G. Q. *ACS Nano* **2010**, *4* (7), 4324−4330.
(14) Lis, H.; Sharon, N. *Chem. Rev.* **1998**, *98* (2), 637−674.
(15) Mammen, M.; Choi, S.-K.; Whitesides, G. M. *Angew. Chem., Int. Ed.* **1998**, *37* (20), 2754−2794.
(16) Jelinek, R.; Kolusheva, S. *Chem. Rev.* **2004**, *104* (12), 5987−6015.
(17) Chen, Q.; Xu, Y. H.; Du, Y. G.; Han, B.-H. *Polymer* **2009**, *50* (13), 2830−2835.
(18) Chen, Q.; Cui, Y.; Zhang, T. L.; Cao, J.; Han, B.-H. *Biomacromolecules* **2010**, *11* (1), 13−19.
(19) Wang, J. Y.; Wang, H. M.; Song, Z. J.; Kong, D. L.; Chen, X. M.; Yang, Z. M. *Colloids Surf., B* **2010**, *180* (2), 155−160.
(20) Bhuniya, S.; Kim, B. H. *Chem. Commun.* **2006**, No. 17, 1842−1844.
(21) Dawn, A.; Fujita, N.; Haraguchi, S.; Sada, K.; Shinkai, S. *Chem. Commun.* **2009**, No. 16, 2100−2102.
(22) Lee, K. Y.; Mooney, D. J. *Chem. Rev.* **2001**, *101* (7), 1869−1880.
(23) Kiyonaka, S.; Sugiyasu, K.; Shinkai, S.; Hamachi, I. *J. Am. Chem. Soc.* **2002**, *124* (37), 10954−10955.
(24) Tian, Y.; Zhang, L.; Duan, P. F.; Liu, F. Y.; Zhang, B. Q.; Liu, C. Y.; Liu, M. H. *New J. Chem.* **2010**, *34* (12), 2847−2852.
(25) Srinivasan, S.; Babu, S. S.; Praveen, V. K.; Ajayaghosh, A. *Angew. Chem., Int. Ed.* **2008**, *47* (31), 5746−5749.
(26) Adhikari, B.; Biswas, A.; Banerjee, A. *Langmuir* **2012**, *28* (2), 1460−1469.
(27) Ahlborn, C.; Siegmund, K.; Richert, C. *J. Am. Chem. Soc.* **2007**, *129* (49), 15218−15232.
(28) Tropper, F. D.; Andersson, F. O.; Braun, S.; Roy, R. *Synthesis* **1992**, No. 7, 618−620.
(29) Lindgren, L. J.; Wang, X. J.; Inganäs, O.; Andersson, M. R. *Synth. Met.* **2005**, *154* (1−3), 97−100.
(30) Zhou, D.; Cheng, Q.-Y.; Han, B.-H. *Carbon* **2011**, *49* (12), 3920−2927.
(31) Stankovich, S.; Piner, R. D.; Chen, X. Q.; Wu, N. Q.; Nguyen, S. T.; Ruoff, R. S. *J. Mater. Chem.* **2006**, *16* (2), 155−158.
(32) von Minden, H. M.; Morr, M.; Milkereit, G.; Heinz, E.; Vill, V. *Chem. Phys. Lipids* **2002**, *114* (1), 55−80.
(33) von Minden, H. M.; Brandenburg, K.; Seydel, U.; Koch, M. H. J.; Garamus, V.; Willumeit, R.; Vill, V. *Chem. Phys. Lipids* **2000**, *106* (2), 157−179.